



Prognostic and immunological role of alpha-L-fucosidase 2 (*FUCA2*) in hepatocellular carcinoma

Yuanhui Hu, Dongling Tang, Pingan Zhang

Department of Laboratory Medicine, Renmin Hospital of Wuhan University, Wuhan, China

Contributions: (I) Conception and design: Y Hu, D Tang; (II) Administrative support: D Tang, P Zhang; (III) Provision of study materials or patients: Y Hu, P Zhang; (IV) Collection and assembly of data: Y Hu, D Tang; (V) Data analysis and interpretation: Y Hu, P Zhang; (VI) Manuscript writing: All authors; (VII) Final approval of manuscript: All authors.

Correspondence to: Pingan Zhang. Renmin Hospital of Wuhan University, No. 238 Jiefang Road, Wuchang District, Wuhan 430060, China. Email: zhangpingan927@163.com.

Background: This study investigated the prognostic and immunological significance of alpha-L-fucosidase 2 (*FUCA2*) in hepatocellular cancer (HCC).

Methods: The expression of *FUCA2* and its clinical and prognostic values were explored across several databases, namely the University of Alabama Cancer Database, The Cancer Genome Atlas, Gene Expression Profiling Interactive Analysis, and the Human Protein Atlas. The prognostic relevance of *FUCA2* was investigated using Kaplan-Meier curves, nomograms, and Cox analysis. The “limma” package in R was used to identify differentially expressed genes between high and low *FUCA2* expression. A protein interaction network was established using the Search Tool for the Retrieval of Interacting Genes (STRING), whereas hub genes and clustering modules were identified using Cytoscape. “clusterProfiler”, an R package, was used to examine the potential function of *FUCA2*. Using gene set enrichment analysis, signaling pathways associated with *FUCA2* expression were identified. Cell-type Identification by Estimating Relative Subsets of RNA Transcripts (CIBERSORT), Tumor Immune Estimation Resource (TIMER) 2.0, and Tumor and Immune System Interaction Database (TISIDB) were used to examine immune infiltration and *FUCA2* in HCC.

Results: Many datasets indicated that *FUCA2* expression is higher in HCC, and that this is related to age and overall survival (OS). With the cutoff value of 50% as the dividing threshold, the patients were divided into a high-*FUCA2* expression group (n=167) and a low-*FUCA2* expression group (n=168). High levels of *FUCA2* expression coincided with decreased OS. *FUCA2* expression in HCC was associated with immune infiltrates. The functional mechanisms of *FUCA2* depend on signal release, extracellular matrix collagen, and neuroactive ligands and receptors.

Conclusions: In HCC, increased *FUCA2* expression is associated with a poor prognosis and immune infiltration. *FUCA2* may serve as an immunological and predictive biomarker for HCC.

Keywords: Alpha-L-fucosidase 2 (*FUCA2*); hepatocellular carcinoma; immune microenvironment; prognosis

Submitted Jul 05, 2022. Accepted for publication Nov 07, 2022. Published online Feb 13, 2023.

doi: 10.21037/tcr-22-1850

View this article at: <https://dx.doi.org/10.21037/tcr-22-1850>

Introduction

Hepatocellular carcinoma (HCC), whose incidence is increasing, is one of the top 5 deadliest illnesses, the seventh most prevalent type of illness in the United States, and the leading cause of cancer-related death worldwide (1,2).

Annually, there are around 841,000 new cases of HCC and 782,000 deaths worldwide, with survival reported to be 6–20 months without treatment globally (3). HCC is the predominant (>90%) form of primary liver cancer, and is very prone to recurrence and dissemination, posing a

significant threat to health (4,5). Recently, there has been considerable progress in the field of tumor immunity research. Immunotherapy provides an unparalleled opportunity to effectively treat cancer by stimulating the immune system to fight tumor development and progression (6,7). Research into HCC immune-associated genes and the immunological microenvironment enhances our knowledge of the mechanisms of carcinogenesis and may serve as a guide for the use of drugs or the development of new treatments (8).

Alpha-L-fucosidase 2 (*FUCA2*) is a member of the glycosyl hydrolase 29 family and has fucosidase activity; nevertheless, very few studies have been conducted so far to determine its function (9). *FUCA2* is responsible for the removal of alpha-1,6-fucose attached to the N-acetylglucosamine residue of glycoproteins. *FUCA2* can be used to identify and treat stomach cancer linked to *Helicobacter pylori* (10). In recent years, it has become apparent that serum *FUCA2* may be a possible biomarker for the early detection of HCC (11). However, the connection between *FUCA2* and HCC prognosis remains unclear. Further research is required to identify the role of *FUCA2* in the genesis and progression of HCC.

Using integrated bioinformatics analysis, it is now possible to evaluate hundreds of relevant genes in several databases simultaneously (12). To the best of our knowledge,

a bioinformatics study has not yet been conducted to determine the unique characteristics of *FUCA2* in HCC. Moreover, it is yet to be determined how *FUCA2* influences the immune microenvironment in HCC. In the present study, we evaluated the significance of *FUCA2* in the genesis and prognosis of HCC by analyzing gene expression, survival status, and immune infiltration correlations across many databases. Using The Cancer Genome Atlas (TCGA) database, we found a high correlation between *FUCA2* expression levels and the clinical features of patients with HCC. Therefore, we examined the signaling pathways associated with *FUCA2* and correlated them with the immune infiltration of *FUCA2* in patients with HCC. The aim of this study was to determine whether *FUCA2* is a unique prognostic biomarker and the likely molecular processes that influence prognosis in liver cancer and thus to provide a theoretical foundation for our upcoming cellular and animal investigations, which we anticipate will advance HCC diagnosis and therapy. We present the following article in accordance with the TRIPOD reporting checklist (available at <https://tcr.amegroups.com/article/view/10.21037/tcr-22-1850/rc>).

Methods

Data collection

Data were collected from TCGA (<https://portal.gdc.cancer.gov/>), which includes RNA sequencing (RNA-seq) data on the expression of *FUCA2* and clinical information from 370 HCC and 50 adjacent nontumor tissues. The relationship between gene expression and survival was evaluated using the R “survival” package (The R Foundation for Statistical Computing; <https://www.rdocumentation.org/packages/survival/versions/3.4-0>), whereas the “rms” package (<https://cran.r-project.org/web/packages/rms/>) was used to predict 1-, 3-, and 5-year survival rates by analyzing different variables. The study was conducted in accordance with the Declaration of Helsinki (as revised in 2013). The study was approved by the Institutional Ethics Board of Renmin Hospital of Wuhan University (No. WDRY2020-K223), and individual consent for this retrospective analysis was waived.

Gene Expression Profiling Interactive Analysis 2 (GEPIA2), Human Protein Atlas (HPA), and the University of Alabama Cancer (UALCAN) database

GEPIA2 integrates TCGA and genotype tissue expression

Highlight box

Key findings

- Increased alpha-L-fucosidase 2 (*FUCA2*) expression is associated with a poor prognosis and immune infiltration of hepatocellular carcinoma (HCC).

What is known and what is new?

- HCC is one of the leading causes of cancer related death worldwide. Research into HCC immune-associated genes and the immunological microenvironment enhances our knowledge of the mechanisms of carcinogenesis.
- We evaluated the significance of *FUCA2* in the genesis and prognosis of HCC by analyzing gene expression, survival status, and immune infiltration correlations across many databases.

What is the implication, and what should change now?

- The implication of this study is that *FUCA2* is a good prognostic biomarker and the likely molecular processes that influence prognosis in HCC. Based on the theoretical foundation this study provides, what should change is the upcoming cellular and animal investigations, which will advance HCC diagnosis and therapy.

data using shared pipelines. GEPIA2 was used in the present study to evaluate pan-cancer *FUCA2* expression, gene association, and overall survival (OS). The HPA contains data on the transcriptomes of over 8,000 patients (13). In the present study, using the HPA, we undertook a proteome analysis using 26,941 antibodies to analyze 17,165 different proteins. The UALCAN database is a popular tool for evaluating genomics data in cancer (14). Using the UALCAN database, we evaluated the association between *FUCA2* messenger RNA (mRNA) and protein levels and clinicopathological markers.

Enrichment analysis

A heat map and volcano plot were created using the pheatmap tool in R. The “ggplot2” R package (<https://cran.r-project.org/web/packages/ggplot2/index.html>) in R 4.1.2 was used to study Gene Ontology (GO), which comprises cellular components, molecular functions, biological processes, and Kyoto Encyclopedia of Genes and Genomes (KEGG) pathway enrichment. The Search Tool for the Retrieval of Interacting Genes (STRING) was used to construct the *FUCA2* protein-protein interaction (PPI) network. The cytoHubba and molecular complex detection (MCODE) Cytoscape plugins were used to identify hub genes in PPI networks (15). Gene set enrichment analysis (GSEA) was used to determine whether changes in gene expression between 2 biological situations (high and low *FUCA2* expressions) were statistically significant (16).

Tumor-infiltrating immune cell analysis

Immune infiltration [B cells, dendritic cells, T cells, macrophages, and natural killer (NK) cells] was investigated using Cell-type Identification by Estimating Relative Subsets of RNA Transcripts (CIBERSORT) (17). Only samples with $P < 0.05$ in CIBERSORT were evaluated. Spearman correlation coefficient was used to compare immune cell types in groups with high and low levels of *FUCA2*. The Tumor Immune Estimation Resource (TIMER) 2.0 website was used to assess pan-cancer gene expression and immune infiltration (18). We further investigated the relationship between *FUCA2* and the infiltration of CD4⁺ T cells, B cells, CD8⁺ T cells, dendritic cells, neutrophils, and macrophages. The Tumor and Immune System Interaction Database (TISIDB) was used to investigate the impact of cancer on the immune system (19).

Statistical analysis

All statistical analyses were conducted using R 4.1.2. Variables were compared between groups using either Fisher exact test or the chi-squared test. Survival was analyzed using Kaplan-Meier curves and was compared between groups using the log-rank test. Univariate and multivariate Cox regression analyses were used to investigate the effect of distinct variables on HCC patient survival. Spearman rank correlation test was used to determine the relationship between 2 variables. Statistical significance was set at a two-sided P value < 0.05 .

Results

FUCA2 transcript levels in patients with HCC

FUCA2 pan-cancer expression was analyzed using GEPIA2 (Figure 1A) and TIMER 2.0 (Figure 1B). Cancers of the breast, esophagus, lungs, stomach, liver, colon, and pancreas expressed *FUCA2* to a greater extent than did other cancers. These results indicate that *FUCA2* is prevalent in HCC. With the cutoff value of 50% (TCGA database; the cutoff value of *FUCA2* expression used to divide groups was 4.791648) as the dividing threshold, the patients were divided into a high-*FUCA2* expression group ($n=167$) and a low-*FUCA2* expression group ($n=168$), and several clinical parameters were evaluated according to *FUCA2* mRNA expression (Table 1). This analysis revealed that *FUCA2* expression is associated with the age at which HCC is diagnosed.

Prognostic value of *FUCA2*

FUCA2 expression was found to be considerably higher in HCC than in adjacent tissues (Figure 2A,2B). As shown in Figure 2C, the median OS of patients with HCC was much longer for those with low *FUCA2* expression than for those with high *FUCA2* expression ($P < 0.001$). These findings suggest that overexpression of *FUCA2* protein decreases the survival rate of individuals with HCC. Certain treatments, such as antibody or short interference RNA, that reduce the amount of *FUCA2* protein in the body may help patients with HCC live longer.

Using univariate and multivariate Cox proportional hazards regression analysis, we reviewed and assessed the clinical parameters that could be possible risk factors. According to univariate Cox regression analysis of the

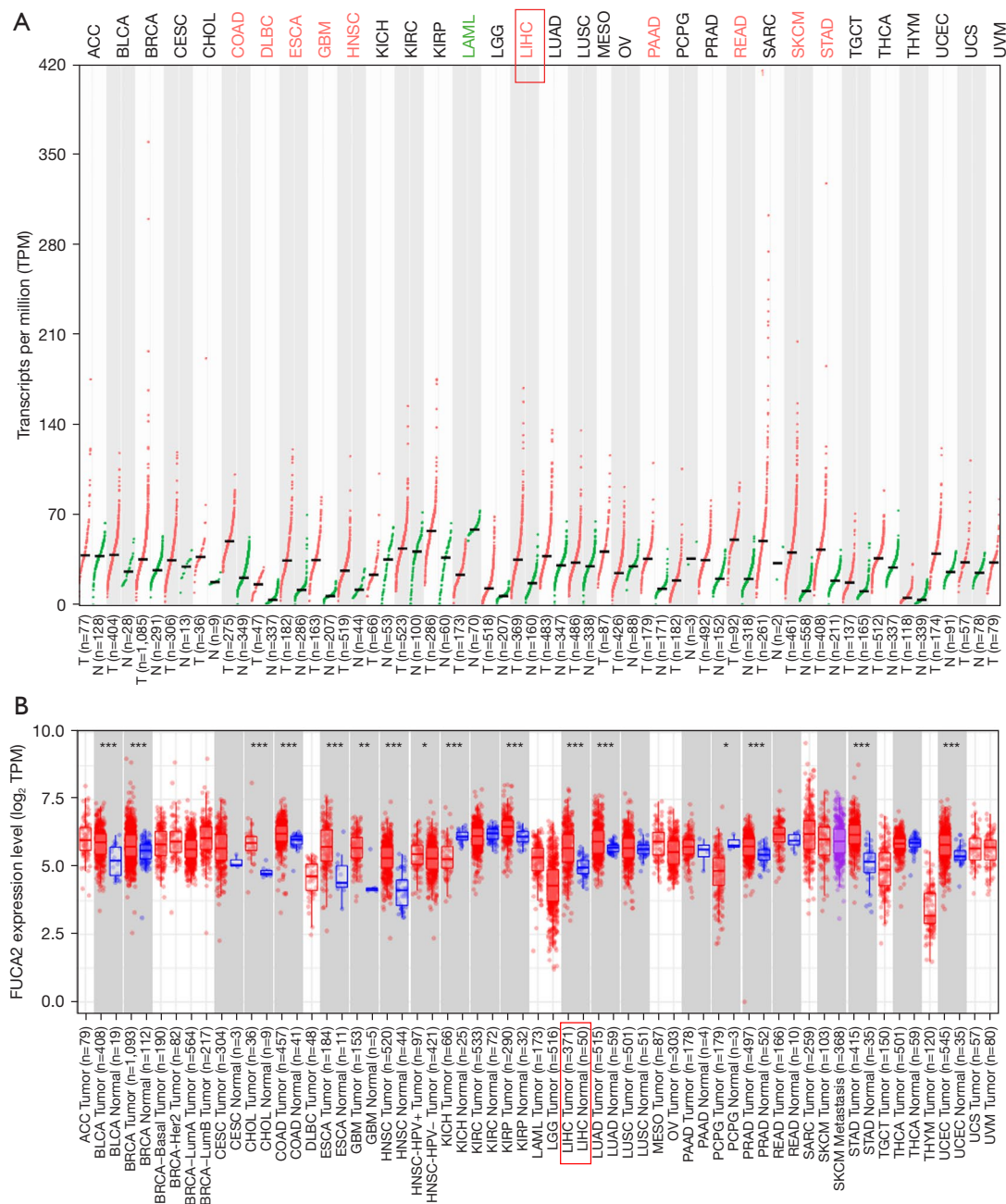


Figure 1 Analysis of *FUCA2* in all tumors. (A) *FUCA2* expression in all malignancies was evaluated using GEPIA2. Red letters indicate elevated *FUCA2* expression, whereas green letters indicate reduced expression. (B) A database study of *FUCA2* in cancer using TIMER 2.0. Red represents HCC. Liver hepatocellular carcinoma was labelled in red box. *, $P < 0.05$; **, $P < 0.01$; ***, $P < 0.001$. *FUCA2*, alpha-L-fucosidase 2; GEPIA2, Gene Expression Profiling Interactive Analysis 2; HCC, hepatocellular carcinoma; TIMER, Tumor Immune Estimation Resource; TPM, transcripts per million; T, tumor; N, normal; ACC, adrenocortical carcinoma; BLCA, bladder urothelial carcinoma; BRCA, breast invasive carcinoma; CESC, cervical squamous cell carcinoma and endocervical adenocarcinoma; CHOL, cholangiocarcinoma; COAD, colon adenocarcinoma; DLBC, lymphoid neoplasm diffuse large B-cell lymphoma; ESCA, esophageal carcinoma; GBM, glioblastoma multiforme; HNSC, head and neck squamous cell carcinoma; KICH, kidney chromophobe; KIRC, kidney renal clear cell carcinoma; KIRP, kidney renal papillary cell carcinoma; LAML, acute myeloid leukemia; LGG, brain lower grade glioma; LIHC, liver hepatocellular carcinoma; LUAD, lung adenocarcinoma; LUSC, lung squamous cell carcinoma; MESO, mesothelioma; OV, ovarian serous cystadenocarcinoma; PAAD, pancreatic adenocarcinoma; PCPG, pheochromocytoma and paraganglioma; PRAD, prostate adenocarcinoma; READ, rectum adenocarcinoma; SARC, sarcoma; SKCM, skin cutaneous melanoma; STAD, stomach adenocarcinoma; TGCT, testicular germ cell tumors; THCA, thyroid carcinoma; THYM, thymoma; UCEC, uterine corpus endometrial carcinoma; UCS, uterine carcinosarcoma; UVM, uveal melanoma.

Table 1 *FUCA2* mRNA expression and clinical features of patients with hepatocellular carcinoma

Variables	<i>FUCA2</i> expression		P value
	High (n=167)	Low (n=168)	
Sex			0.534
Female	57 (34.1)	51 (30.4)	
Male	110 (65.9)	117 (69.6)	
Age (years)			0.0149
<40	23 (13.8)	9 (5.4)	
≥40	144 (86.2)	159 (94.6)	
Stage			0.836
I	80 (47.9)	87 (51.8)	
II	43 (25.7)	41 (24.4)	
III	42 (25.1)	37 (22.0)	
IV	2 (1.2)	3 (1.8)	
T classification			0.766
T1	82 (49.1)	87 (51.8)	
T2	43 (25.7)	43 (25.6)	
T3	39 (23.4)	33 (19.6)	
T4	3 (1.8)	5 (3.0)	
M classification			0.384
M0	133 (79.6)	125 (74.4)	
M1	1 (0.6)	3 (1.8)	
MX	33 (19.8)	40 (23.8)	
N classification			0.52
N0	124 (74.3)	122 (72.6)	
N1	3 (1.8)	1 (0.6)	
NX	40 (24.0)	45 (26.8)	
Residual tumor			0.523
R0	151 (90.4)	151 (89.9)	
R1	4 (2.4)	7 (4.2)	
R2	0 (0)	1 (0.6)	
RX	12 (7.2)	9 (5.4)	
Overall survival			0.058
Yes	64 (38.3)	47 (28.0)	
No	103 (61.7)	121 (72.0)	

Unless indicated otherwise, data are presented as n (%). With the cutoff value of 50% as the dividing threshold, the patients were divided into a high-*FUCA2* expression group (n=167) and a low-*FUCA2* expression group (n=168). *FUCA2*, alpha-L-fucosidase 2.

data, the following factors could contribute to predicting patient survival: age, sex, race, stage, *FUCA2* expression, T, N, and M classification, and residual tumor. The forest plot in *Figure 3A* shows the hazard ratios (HRs) for the clinical characteristics, with “Coef” >0 indicating that these parameters are factors affecting survival in HCC. The overall P value was 3.9026×10^{-8} , and the model had a concordance index (C-index) of 0.7 (*Figure 3A*).

The outcomes of multivariate studies using stepwise models that included the significant risk identified in univariate analyses showed that *FUCA2*, M classification, and residual tumor were independent predictors of HCC survival (*Figure 3B*). The overall P value was 1.5418×10^{-5} , and the model had a C-index of 0.66 (*Figure 3B*). In the multivariate Cox regression analysis, the HRs for *FUCA2*, M classification, and residual tumor were 1.74 [95% confidence interval (CI): 1.31–2.30; $P < 0.001$], 1.25 (95% CI: 1.00–1.56; $P = 0.0478$), and 1.30 (95% CI: 1.01–1.68; $P = 0.0453$), respectively (*Figure 3B*).

We created a nomogram that uses age and sex to predict the chances of survival at 1 and 2 years for patients with HCC, with each component allocated proportional points according to its influence on survival (*Figure 3C*).

Correlations between *FUCA2* expression and clinical features

Using the UALCAN database, the relationships between *FUCA2* expression and clinical characteristics in patients with HCC were investigated. First, *FUCA2* expression was higher in HCC than in normal tissues (*Figure 4A*; $P = 1.62 \times 10^{-12}$). In addition, compared with normal tissues, *FUCA2* expression was higher in HCC stages 1, 2, and 3 ($P = 1.62 \times 10^{-12}$, $P = 2.24 \times 10^{-10}$, and $P = 2.75 \times 10^{-11}$, respectively; *Figure 4B*). *FUCA2* expression in HCC stage 4 did not differ significantly from that in other HCC stages or normal tissues (*Figure 4B*). *FUCA2* expression was higher in the Caucasian, African American, and Asian groups than in the normal group ($P = 1.62 \times 10^{-12}$, $P = 3.77 \times 10^{-4}$, and $P < 1 \times 10^{-12}$, respectively; *Figure 4C*). There was no significant difference in *FUCA2* expression in HCC samples between males and females ($P > 0.05$; *Figure 4D*). Compared with normal tissues, *FUCA2* expression was significantly higher in samples from patients with HCC aged 21–40, 41–60, and 61–80 years ($P = 1.79 \times 10^{-4}$, $P = 1.62 \times 10^{-12}$, and $P = 1.62 \times 10^{-12}$), but not in those aged 81–100 years (*Figure 4E*). In addition, compared with normal tissues, *FUCA2* expression was significantly

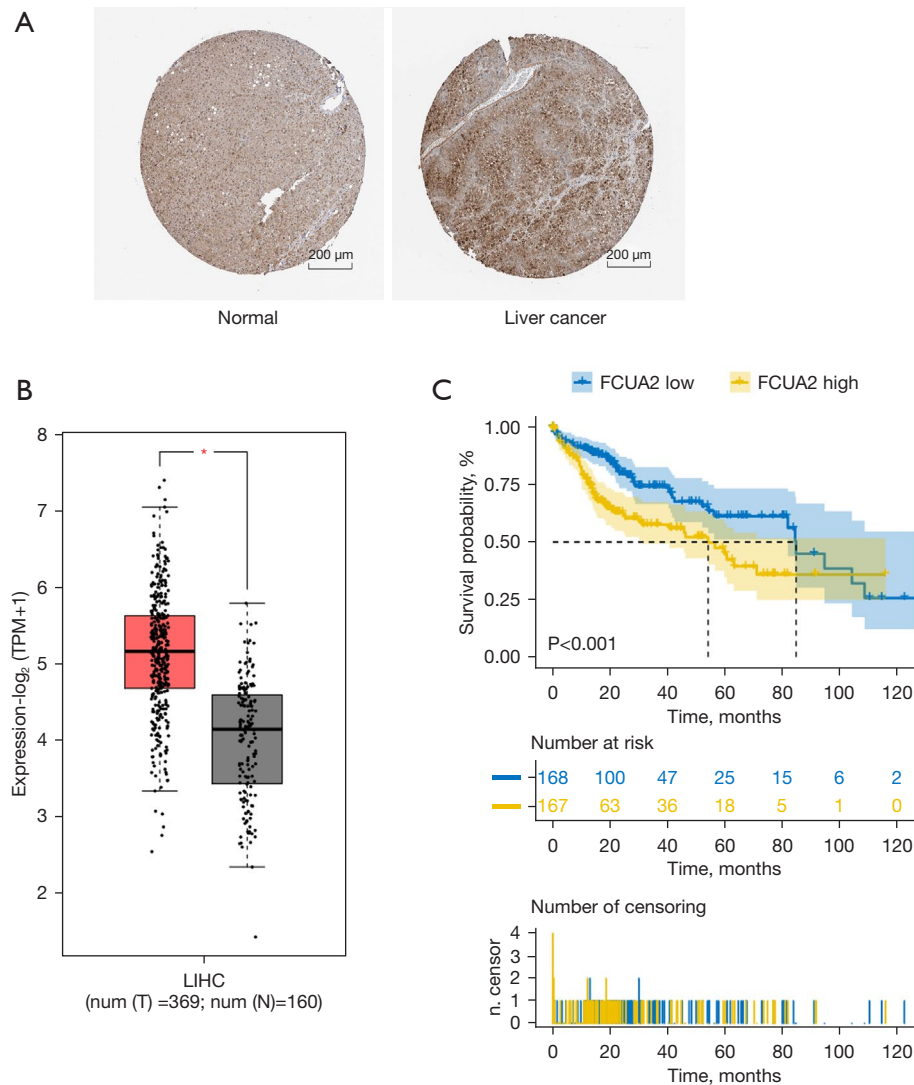


Figure 2 Increased *FUCA2* expression in HCC tissue. (A) Images of immunohistochemical staining results using an anti-*FUCA2* antibody from the Human Protein Atlas. *FUCA2* was stained brown in granules. Scale bars =200 μ m. (B) Scatter plot of *FUCA2* expression in normal (gray) and malignant liver (HCC; red) tissue. *, $P < 0.05$. (C) Correlation between *FUCA2* expression and HCC survivability. *FUCA2*, alpha-L-fucosidase 2; HCC, hepatocellular carcinoma; LIHC, liver hepatocellular carcinoma; num, number; TPM, transcripts per million; T, tumor; N, normal.

higher in all weight categories (normal, extreme, obese, and extremely obese ($P < 1 \times 10^{-12}$, $P = 1.16 \times 10^{-8}$, $P = 1.06 \times 10^{-7}$, and $P = 3.12 \times 10^{-2}$, respectively; *Figure 4F*) and all tumor grades (1, 2, 3, and 4; $P = 6.04 \times 10^{-5}$, $P = 3.33 \times 10^{-15}$, $P < 1 \times 10^{-12}$, $P = 4.93 \times 10^{-2}$, respectively; *Figure 4G*). *FUCA2* expression did not differ significantly between the N0 and N1 group ($P > 0.05$; *Figure 4H*). *FUCA2* expression was significantly higher in both the tumor protein p53 (*TP53*) mutant and nonmutant groups than in the normal group (both $P < 1 \times 10^{-12}$) and higher in the *TP53* mutant group than in the

nonmutant group ($P = 4.91 \times 10^{-8}$; *Figure 4I*). Finally, *FUCA2* expression was significantly higher in samples of HCC, fibrolamellar carcinoma, and hepatocholangiocarcinoma (mixed) than in normal tissues ($P < 1 \times 10^{-12}$, $P = 2.22 \times 10^{-2}$, $P = 1.42 \times 10^{-7}$; *Figure 4J*).

Analysis of the enrichment of FUCA2-related pathways

To explore the potential mechanism by which *FUCA2* causes tumor progression, we analyzed differentially

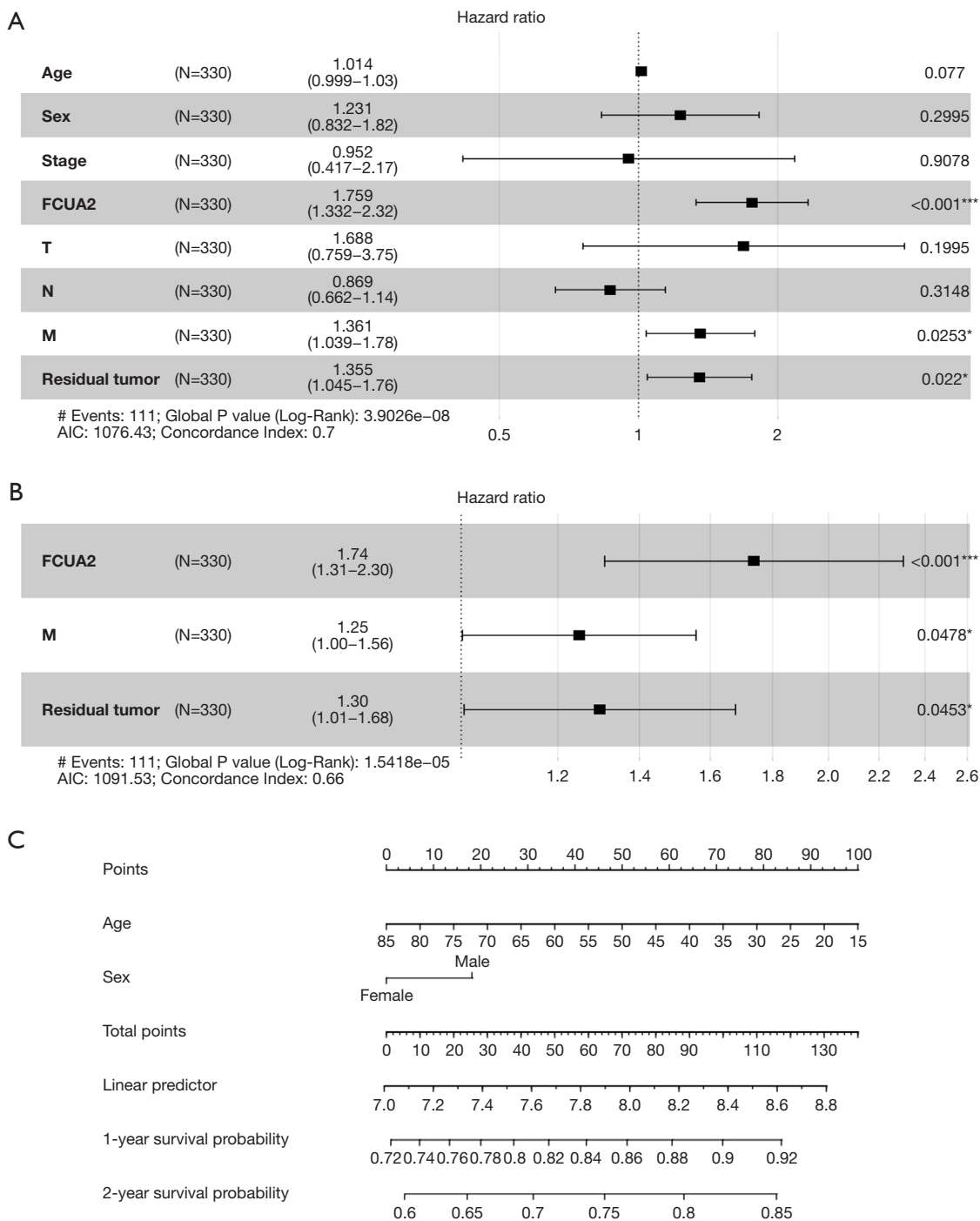


Figure 3 Clinical data, Cox regression analysis, and nomogram validation. Forest plots using univariate (A) and multivariate (B) Cox regression. *, P<0.05; ***, P<0.001. (C) The nomogram combined sex and age. AIC, Akaike information criterion; FCUA2, alpha-L-fucosidase 2.

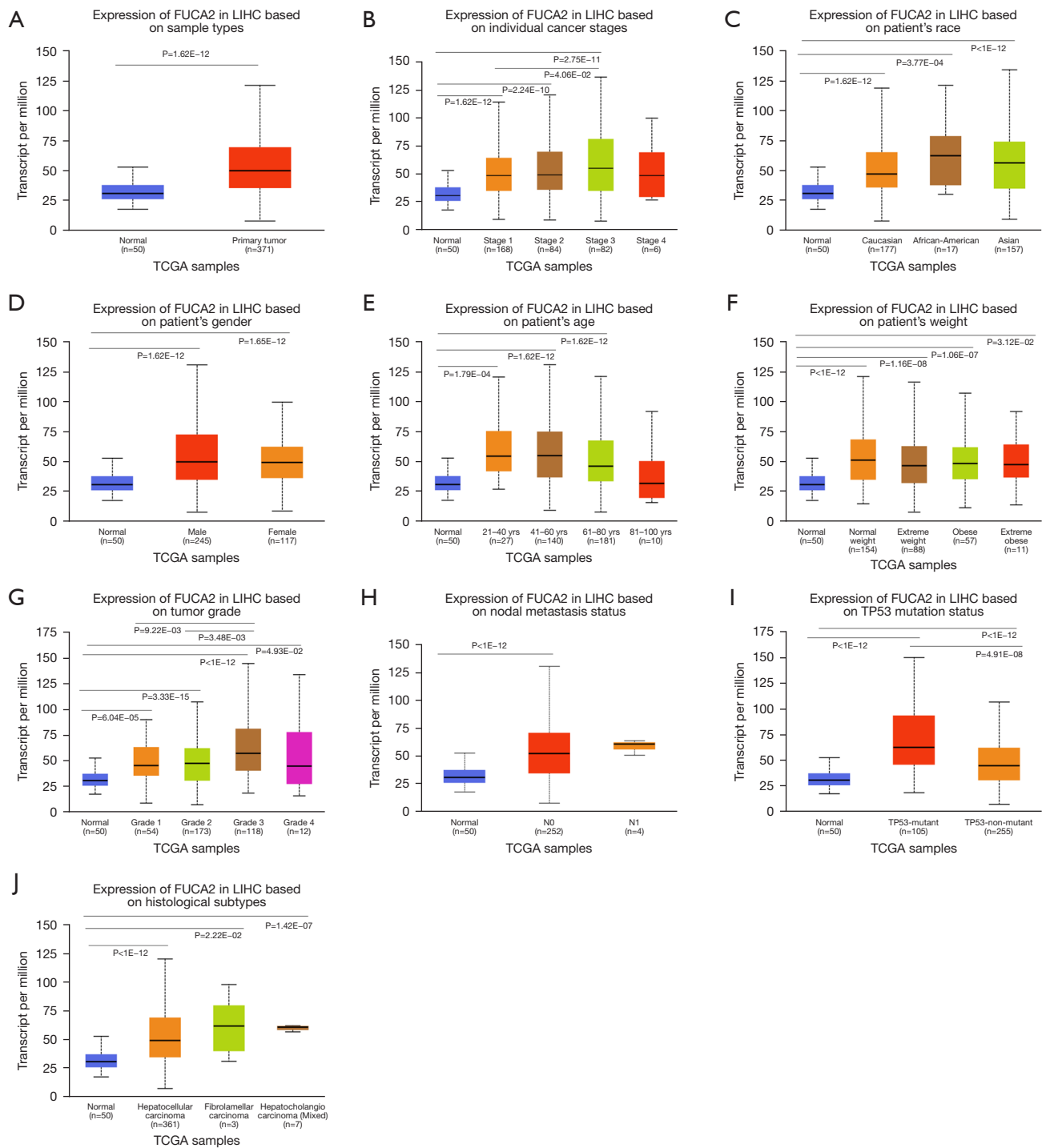


Figure 4 Box plots analyzing *FUCA2* expression in patients with HCC according to different features: (A) overall expression; (B) stage; (C) race; (D) sex; (E) age; (F) weight; (G) grade; (H) node metastasis; (I) TP53 mutation; (J) histological subtype. With the UALCAN database, these datasets were evaluated in their entirety. The boxes show the interquartile range, with the median value indicated by the horizontal line; the whiskers show the range. *FUCA2*, alpha-L-fucosidase 2; HCC, hepatocellular carcinoma; LIHC, liver hepatocellular carcinoma; TCGA, The Cancer Genome Atlas; TP53, tumor protein p53; UALCAN, University of Alabama Cancer Database.

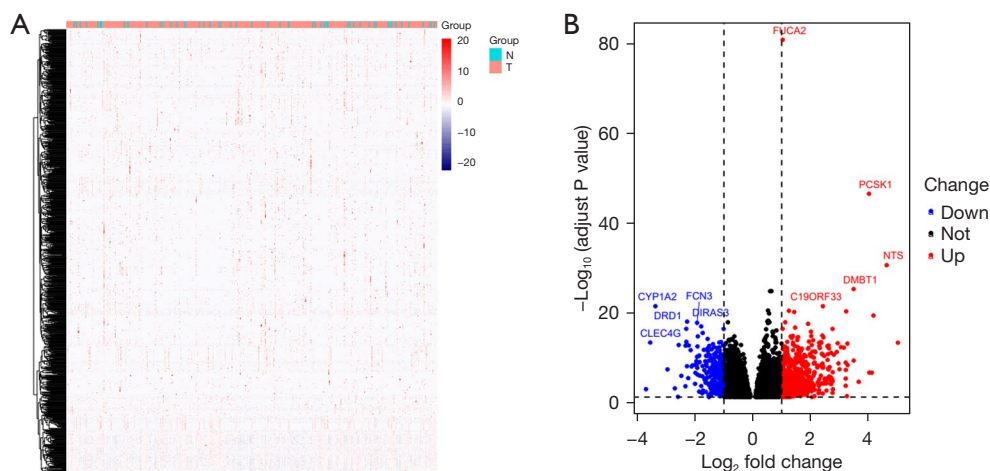


Figure 5 Screening for DEGs. (A) DEGs were organized hierarchically. Each row represents a DEG, whereas each column is a sample: orange indicates HCC samples and blue indicates normal tissues. The horizontal and vertical axes show the sample and protein clustering, respectively. Red indicates upregulation of gene expression, and blue indicates downregulation. (B) Volcano plot. Red dots represent upregulated genes (\log_2 FC > 1 , $P < 0.05$). Blue dots represent suppressed genes (\log_2 FC < -1 , $P < 0.05$). DEGs, differentially expressed genes; FC, fold change; HCC, hepatocellular carcinoma.

expressed genes (DEGs) between the high- and low-*FUCA2* expression groups using a heat map and volcano plots (Figure 5A, 5B). A clustering heat map was constructed of genes whose expression levels varied across samples, with the horizontal and vertical axes, respectively, reflecting sample and protein clustering (Figure 5A). The heat map was separated into 2 categories of tumor tissue and adjacent normal tissue, with red indicating the upregulation of gene expression and blue indicating the downregulation. The volcano plots provide an integral overview of differentially expressed genes (Figure 5B).

The DEGs identified were analyzed for enrichment of GO terms and KEGG pathways. The following biological processes were markedly affected by the level of *FUCA2* expression: signal release, response to xenobiotic stimulus, and organic anion transport (Figure 6A). The most enriched cellular component terms were collagen-containing extracellular matrix, apical part of cell, and apical plasma membrane (Figure 6B). In terms of molecular function, signaling receptor activator activity, receptor ligand activity, and serine hydrolase activity were the most enriched phrases (Figure 6C). For KEGG terms, neuroactive ligand–receptor interaction, cyclic adenosine monophosphate (cAMP) signal pathway, and chemical carcinogenesis–receptor activation were the most enriched pathways (Figure 6D).

According to the median value of *FUCA2* expression, data were separated into high and low expression sets,

and signaling pathways were evaluated using GSEA. Enriched signaling pathways were chosen on the basis of the normalized enrichment score, the false discovery rate (FDR) Q value, and nominal P value (Figure 6E). There were 10 enriched and cancer-related functions: fatty acid metabolic process, gamete generation process, icosanoid metabolic process, long chain fatty acid metabolic process, monocarboxylic acid metabolic process, organic acid metabolic process, small molecule biosynthetic process, molecule metabolic process, oxidoreductase activity, and oxidoreductase activity acting on paired donors with incorporation or reduction of molecular oxygen (Figure 6E).

Protein interaction network

To further study the interactions between the chosen DEGs, we submitted them to the STRING database. There were 71 nodes and 450 edges in the network (Figure 7A). Based on the Cytoscape cytoHubba plug-in, the 10 most significant hub genes were determined to be galactosidase beta 1 (*GLB1*), hexokinase 1 (*HK1*), hexokinase 2 (*HK2*), hexokinase 3 (*HK3*), glucokinase (*GCK*), lactase (*LCT*), aldo-keto reductase family 1 member B (*AKR1B1*), glucose-6-phosphatase catalytic subunit (*G6PC*), hexokinase domain containing 1 (*HKDC1*), and glucose-6-phosphatase catalytic subunit 2 (*G6PC2*) (Figure 7B). Figure 7C–7F shows the Cytoscape plugin MCODE module analysis

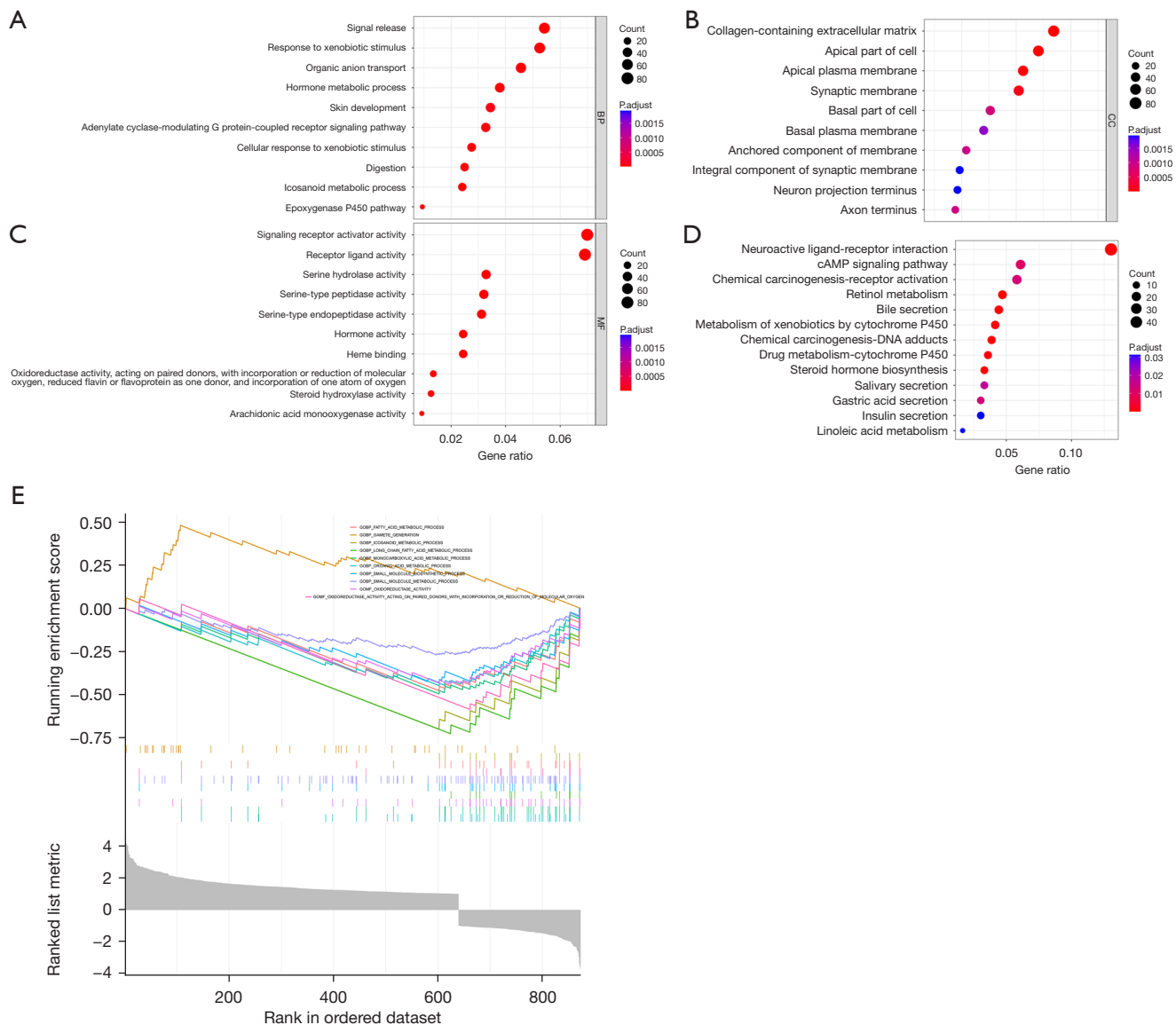


Figure 6 Genes expressed with *FUCA2* in HCC. (A-C) Gene Ontology biological process (A), cellular component (B), and molecular function (C). (D) KEGG pathway analysis. (E) Gene set enrichment analysis for *FUCA2*-expressing samples. *FUCA2*, alpha-L-fucosidase 2; HCC, hepatocellular carcinoma; KEGG, Kyoto Encyclopedia of Genes and Genomes; cAMP, cyclic adenosine monophosphate.

of the PPI networks. *HKDC1*, *LCT*, *HK3*, *G6PC*, *GLB1*, *G6PC2*, *GCK*, aldo-keto reductase family 1 member B10 (*AKR1B10*), maltase-glucoamylase (*MGAM*), galactose mutarotase (*GALM*), *HK2*, *AKR1B1*, glucose-6-phosphatase catalytic subunit 3 (*G6PC3*), *HK1*, and sucrase-isomaltase (*SI*) were the hub nodes with the highest score (13.875) in module 1 (15 nodes, 97 edges; *Figure 7C*), followed by module 2 (8 nodes, 18 edges, score 5.143), module 3 (14 nodes, 32 edges, score 4.923), and module 4 (11 nodes, 20 edges, score 4; *Figure 7D-7F*).

Immune infiltration and correlations with *FUCA2* expression

The heat maps also revealed positive associations between *FUCA2* and the top 5 genes in every kind of cancer (*Figure 7G*). The top 100 *FUCA2*-associated genes were identified with the GEPIA2 database. The associated heat map demonstrated a favorable connection between *FUCA2* and the top 5 genes across a number of cancer types (*Figure 7G*). In addition, *FUCA2* interacted with

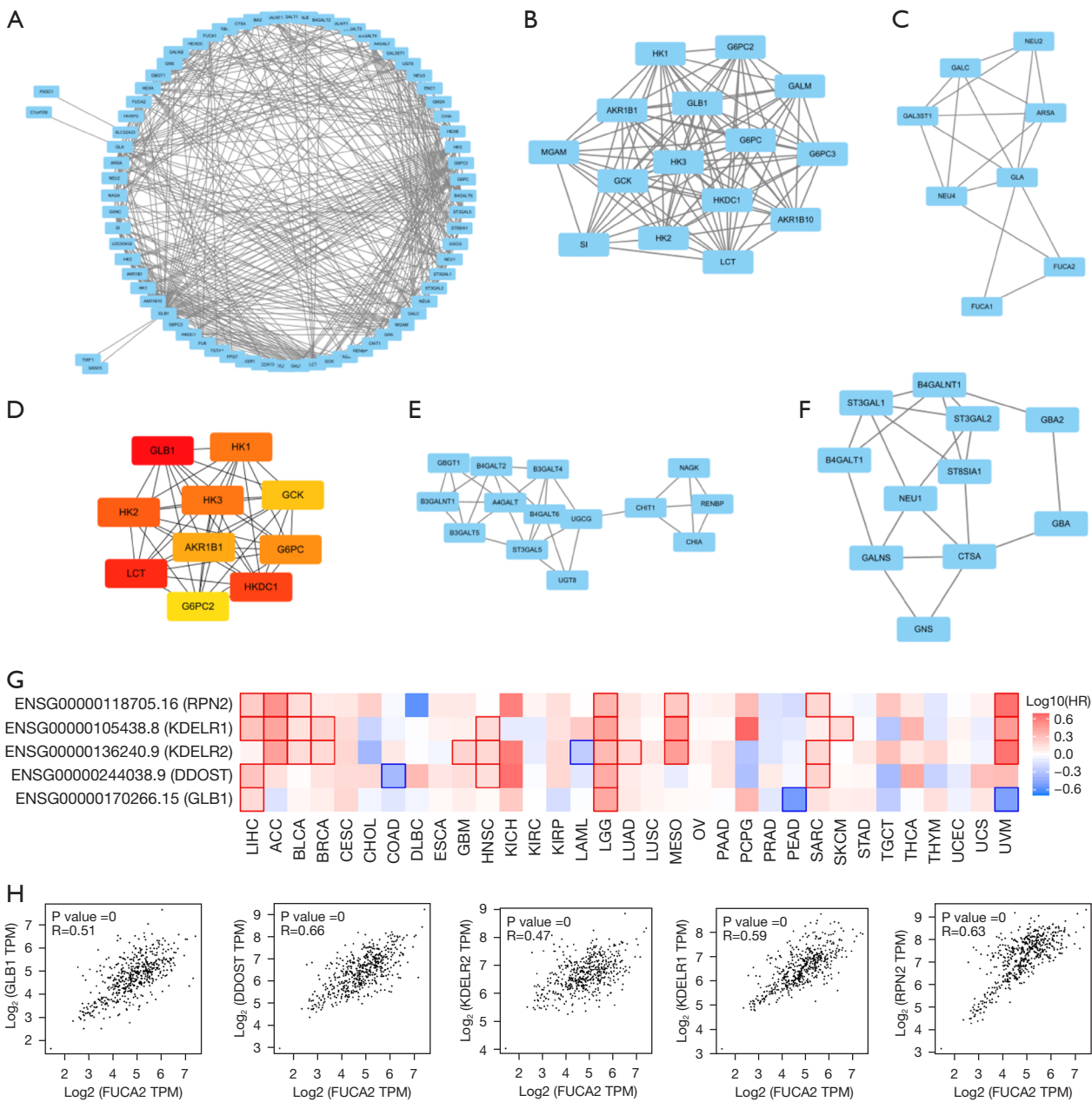


Figure 7 *FUCA2* enrichment gene analysis. (A) *FUCA2*-binding proteins identified using the STRING. (B) The 10 most important hub genes based on Cytoscape cytoHubba. (C-F) The MCODE plug-in for Cytoscape analysis of PPI networks. (G) A heat map pertaining to HCC. (H) Relationship between *FUCA2* and the expression of the top 5 genes (*GLB1*, *DDOST*, *KDELR2*, *KDELR1*, and *RPN2*). *FUCA2*, alpha-L-fucosidase 2; HCC, hepatocellular carcinoma; MCODE, molecular complex detection; PPI, protein-protein interaction; STRING, Search Tool for the Retrieval of Interacting Genes; TPM, transcripts per million; LIHC, liver hepatocellular carcinoma; ACC, adrenocortical carcinoma; BRCA, breast invasive carcinoma; CESC, cervical squamous cell carcinoma and endocervical adenocarcinoma; CHOL, cholangiocarcinoma; COAD, colon adenocarcinoma; DLBC, lymphoid neoplasm diffuse large B-cell lymphoma; ESCA, esophageal carcinoma; GBM, glioblastoma multiforme; HNSC, head and neck squamous cell carcinoma; KICH, kidney chromophobe; KIRC, kidney renal clear cell carcinoma; KIRP, kidney renal papillary cell carcinoma; LAML, acute myeloid leukemia; LGG, brain lower grade glioma; LUAD, lung adenocarcinoma; LUSC, lung squamous cell carcinoma; MESO, mesothelioma; OV, ovarian serous cystadenocarcinoma; PAAD, pancreatic adenocarcinoma; PCPG, pheochromocytoma and paraganglioma; PRAD, prostate adenocarcinoma; READ, rectum adenocarcinoma; SARC, sarcoma; SKCM, skin cutaneous melanoma; STAD, stomach adenocarcinoma; TGCT, testicular germ cell tumors; THCA, thyroid carcinoma; THYM, thymoma; UCEC, uterine corpus endometrial carcinoma; UCS, uterine carcinosarcoma; UVM, uveal melanoma.

GLB1, dolichyl-diphosphooligosaccharide--protein glycosyltransferase noncatalytic subunit (*DDOST*), KDEL endoplasmic reticulum protein retention receptor 2 (*KDEL2*), KDEL endoplasmic reticulum protein retention receptor 1 (*KDEL1*), and ribophorin II (*RPN2*) in this mode (Figure 7H).

Using CIBERSORT, we next assessed the fractions of tumor-infiltrating immune cells to confirm the link between *FUCA2* expression and the immunological tumor microenvironment. The percentage of each of the 22 types of immune cells in HCC tissues was determined (Figure 8A). The connection between immune infiltration and *FUCA2* expression was computed using TIMER 2.0. As shown in Figure 8B, *FUCA2* expression was correlated with CD4⁺ T cells, B cells, CD8⁺ T cells, dendritic cells, neutrophils, and macrophage infiltration. The TISIDB database analyzed the connection between *FUCA2* and 28 tumor-infiltrating lymphocytes (TILs), revealing that *FUCA2* was associated with TILs in most malignancies (Figure 9A). Figure 9B shows the correlation between *FUCA2* expression and 15 of the 28 TILs in HCC.

Discussion

HCC is one of the most difficult-to-treat and fatal cancers (20). Identifying potential biomarkers may contribute to precise prognostic evaluation and guide systemic therapy in patients with HCC. Various studies have sought prognostic biomarkers (21,22). According to previous studies, esophageal squamous cell carcinoma and gastric cancer are among the malignancies in which *FUCA2* mRNA is expressed at elevated levels (10,23). In accordance with these results, we observed higher *FUCA2* mRNA expression in HCC. Because of this, it is now possible that *FUCA2* is a target molecule in HCC. Furthermore, through analyzing *FUCA2* mRNA expression according to different clinical characteristics, it was found that *FUCA2* expression (TCGA database) is associated with the age at which the patients were diagnosed with HCC. Moreover, higher *FUCA2* mRNA expression predicted a poor prognosis and was an independent factor influencing OS.

The poor prognosis of HCC is a concern globally, and the recurrence and spread of the tumor are significant prognostic variables. There is a strong relationship between cancer stem cells (CSCs) and both tumor recurrence and metastasis. CSCs can both self-replicate to create extra stem cells and differentiate into cancerous cells that are distinct from themselves (24). These CSCs that are able to withstand

therapy will initiate the process of tumor growth (25). It is essential to have complete knowledge of human malignancies to identify particular targets or characteristics for more accurate and individualized therapy (26).

The heat map in Figure 7D shows the coexpression and correlation of the 5 genes most positively associated with *FUCA2*: *GLB1*, *DDOST*, *KDEL2*, *KDEL1*, and *RPN2*. In the TIMER 2.0 database, these genes had a positive connection with *FUCA2* across most cancer types. Overall, the *FUCA2* gene and the *GLB1*, *DDOST*, *KDEL2*, *KDEL1*, and *RPN2* genes may serve as indicators for the prognosis of HCC. According to the PPI networks, *GLB1*, *HK1*, *GCK*, *G6PC*, *HKDC1*, *G6PC2*, *LCT*, *HK2*, *HK3*, and *AKR1B1* are the top 10 hub genes associated with the expression of *FUCA2* in HCC (Figure 7B). According to the findings of the GO analysis, most of these genes are involved in signal release and the creation of collagen-containing extracellular matrix. KEGG analysis determined that the functional activities of *FUCA2* include the interaction of neuroactive ligands and receptors, as well as the cAMP signaling pathway.

Previous studies have established that disruption of the tumor immune microenvironment is a leading driver of cancer development (27). Immune cells that infiltrate the tumor affect the microenvironment and behavior of the tumor. By changing immune cell proportions, *FUCA2* may affect the tumor microenvironment, hence promoting tumor growth and spread. Our study demonstrated a connection between macrophages and *FUCA2* expression. Tumor-associated macrophages have several roles in cancer etiology (28). The control of the tumor microenvironment is complex, and CD4⁺ T cells, B cells, CD8⁺ T cells, dendritic cells, neutrophils, and macrophages may influence the survival of tumor cells. Future studies are needed to determine how *FUCA2* expression affects these cells.

Finally, we identified *FUCA2*-binding proteins and associated genes in cancer. We found that *FUCA2* is overexpressed in HCC, suggesting that *FUCA2* can predict and be used to evaluate the prognosis of HCC patients independently. The results of this study show that *FUCA2* interacts with invading immune cells and linked genes in HCC, which contributes to its association with a poor prognosis in patients with HCC. However, this study focused on clinical relevance and did not investigate the molecular process. Future research will be undertaken *in vivo* and *in vitro* to investigate the *FUCA2*-related pathogenic mechanism of HCC. The findings suggest that *FUCA2* may be a potential target of cancer treatment.

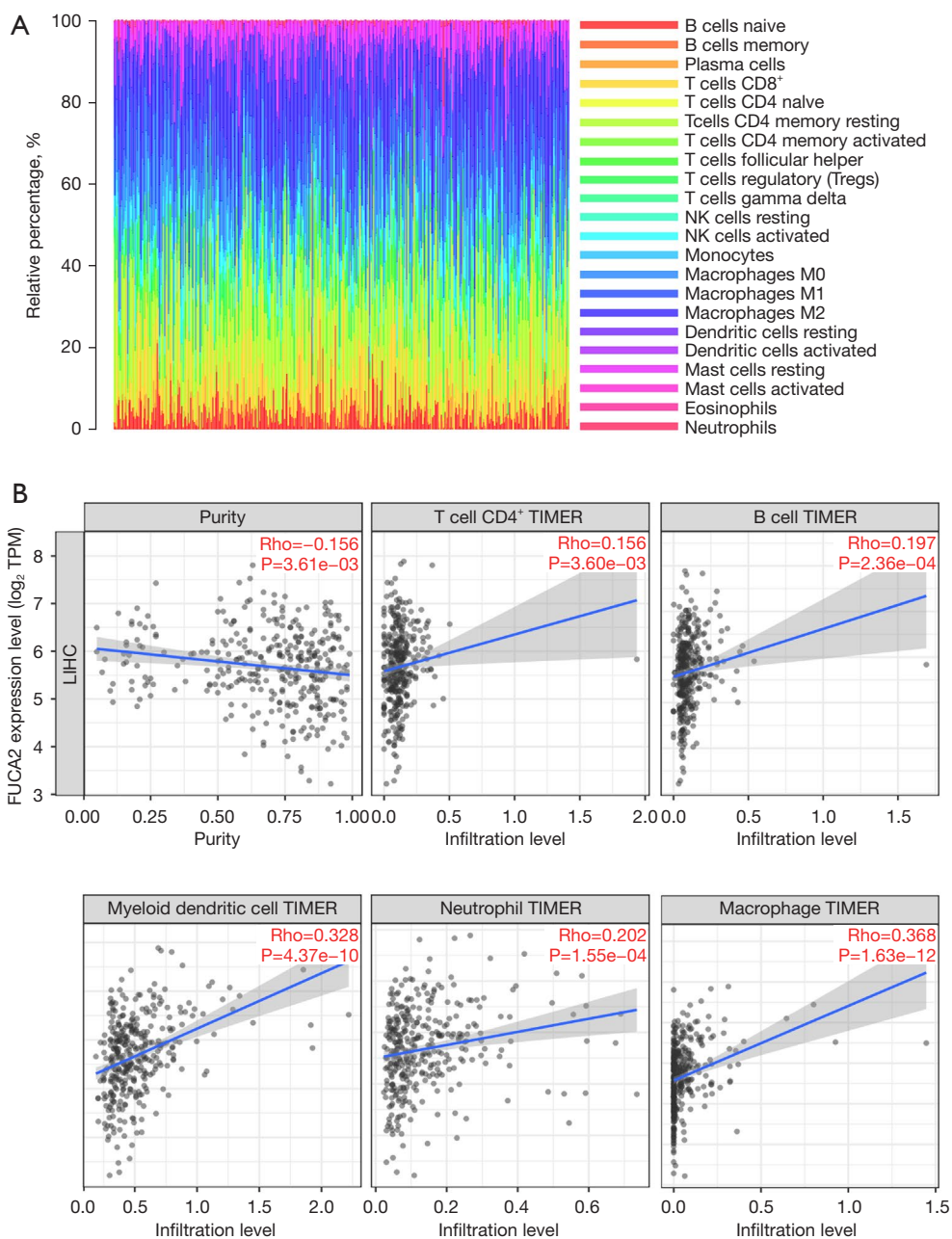


Figure 8 *FUCA2* and immune infiltration in HCC. (A) CIBERSORT calculated the proportions of 22 TIICs per sample. (B) *FUCA2* expression was negatively associated with tumor purity but positively associated with infiltration of CD4⁺ T cells, B cells, CD8⁺ T cells, dendritic cells, neutrophils, and macrophages. CIBERSORT, Cell-type Identification by Estimating Relative Subsets of RNA Transcripts; *FUCA2*, alpha-L-fucosidase 2; HCC, hepatocellular carcinoma; LIHC, liver hepatocellular carcinoma; TIICs, tumor-infiltrating immune cells; TIMER, Tumor Immune Estimation Resource; TPM, transcripts per million.

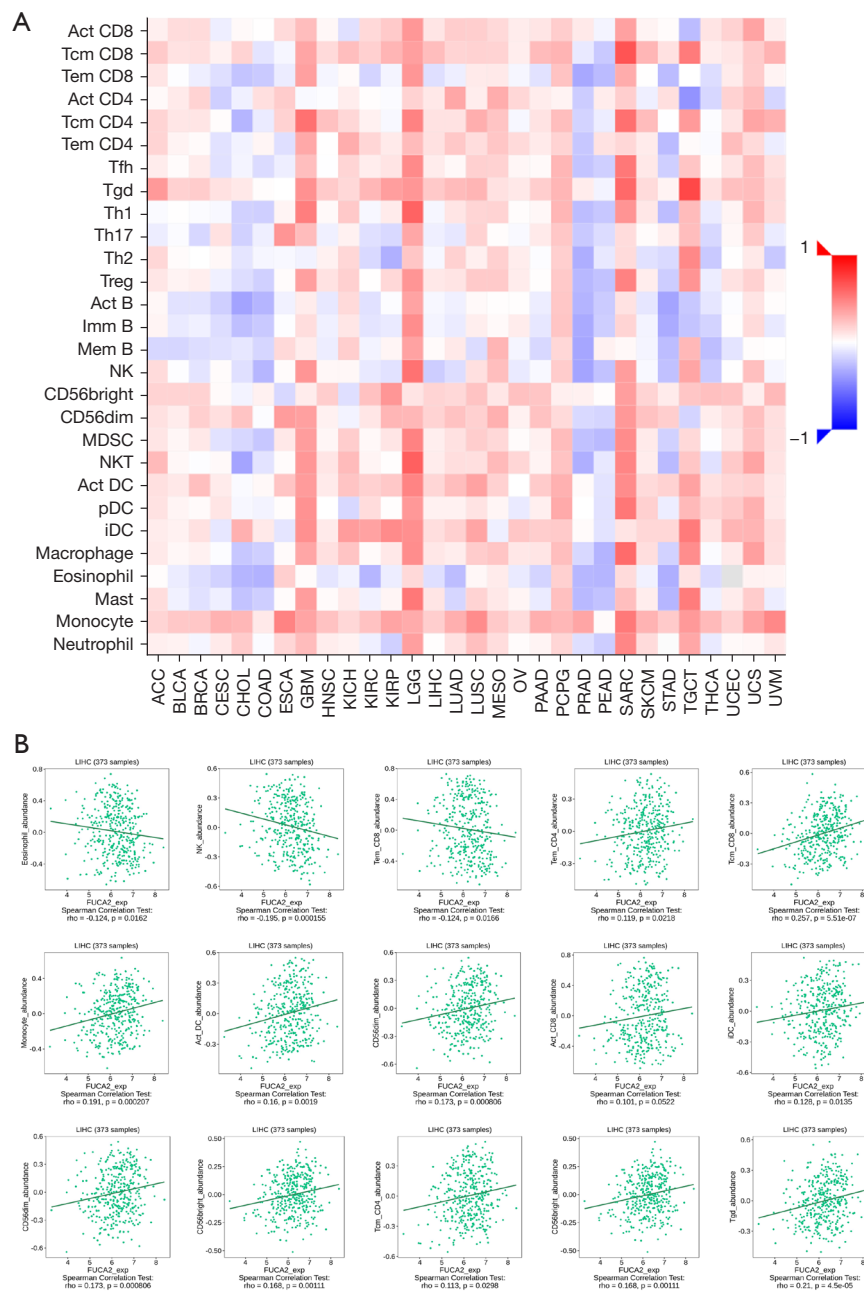


Figure 9 TISIDB study of *FUCA2* expression in different malignancies using TILs. (A) Expression of *FUCA2* and TILs in pan-cancer. (B) *FUCA2* and TILs have a connection to HCC. *FUCA2*, alpha-L-fucosidase 2; HCC, hepatocellular carcinoma; TILs, tumor-infiltrating immune cells; TISIDB, Tumor and Immune System Interaction Database; Act, activated; Tcm, central memory T cell; Tem, effector memory T cell; Tfh, T follicular helper cell; Tgd, gamma delta T cell; Treg, regulatory T cells; Imm, immature; Mem, memory; NK, natural killer; MDSC, myeloid derived suppressor cell; NKT, natural killer T; DC, dendritic cell; pDC, plasmacytoid dendritic cell; iDC, immature dendritic cell; ACC, adrenocortical carcinoma; BLCA, bladder urothelial carcinoma; BRCA, breast invasive carcinoma; CESC, cervical squamous cell carcinoma and endocervical adenocarcinoma; CHOL, cholangiocarcinoma; COAD, colon adenocarcinoma; ESCA, esophageal carcinoma; GBM, glioblastoma multiforme; HNSC, head and neck squamous cell carcinoma; KICH, kidney chromophobe; KIRC, kidney renal clear cell carcinoma; KIRP, kidney renal papillary cell carcinoma; LGG, brain lower grade glioma; LIHC, liver hepatocellular carcinoma; LUAD, lung adenocarcinoma; LUSC, lung squamous cell carcinoma; MESO, mesothelioma; OV, ovarian serous cystadenocarcinoma; PAAD, pancreatic adenocarcinoma; PCPG, pheochromocytoma and paraganglioma; PRAD, prostate adenocarcinoma; PEAD, rectum adenocarcinoma; SARC, sarcoma; SKCM, skin cutaneous melanoma; STAD, stomach adenocarcinoma; TGCT, testicular germ cell tumors; THCA, thyroid carcinoma; THYM, thymoma; UCEC, uterine corpus endometrial carcinoma; UCS, uterine carcinosarcoma; UVM, uveal melanoma.

Conclusions

In summary, *FUCA2* may exert a vital regulatory part in tumor immune cell infiltration, which is also a significant prognostic biomarker for hepatocellular carcinoma, and may become a promising novel and therapeutic target in hepatocellular carcinoma. Besides, our study requires more exploratory research in bioinformatics, and more basic research is needed to verify these outcomes in the future.

Acknowledgments

We would like to express our gratitude to the UCSC, TCGA, and TIMER databases for their contributions to the Cancer Genomics project.

Funding: This research was funded by the National Natural Science Foundation of China (No. 81773444).

Footnote

Reporting Checklist: The authors have completed the TRIPOD reporting checklist. Available at <https://tcr.amegroupp.com/article/view/10.21037/tcr-22-1850/rc>

Conflicts of Interest: All authors have completed the ICMJE uniform disclosure form (available at <https://tcr.amegroupp.com/article/view/10.21037/tcr-22-1850/coif>). The authors have no conflicts of interest to declare.

Ethical Statement: The authors are accountable for all aspects of the work in ensuring that questions related to the accuracy or integrity of any part of the work are appropriately investigated and resolved. The study was conducted in accordance with the Declaration of Helsinki (as revised in 2013). The study was approved by the Institutional Ethics Board of Renmin Hospital of Wuhan University (No. WDRY2020-K223), and individual consent for this retrospective analysis was waived.

Open Access Statement: This is an Open Access article distributed in accordance with the Creative Commons Attribution-NonCommercial-NoDerivs 4.0 International License (CC BY-NC-ND 4.0), which permits the non-commercial replication and distribution of the article with the strict proviso that no changes or edits are made and the original work is properly cited (including links to both the formal publication through the relevant DOI and the license). See: <https://creativecommons.org/licenses/by-nc-nd/4.0/>.

References

1. Siegel RL, Miller KD, Fuchs HE, et al. Cancer statistics, 2022. *CA Cancer J Clin* 2022;72:7-33.
2. Xia C, Dong X, Li H, et al. Cancer statistics in China and United States, 2022: profiles, trends, and determinants. *Chin Med J (Engl)* 2022;135:584-90.
3. Shuai Y, Fan E, Zhong Q, et al. CDCA8 as an independent predictor for a poor prognosis in liver cancer. *Cancer Cell Int* 2021;21:159.
4. Arvanitakis K, Koletsis T, Mitroulis I, et al. Tumor-Associated Macrophages in Hepatocellular Carcinoma Pathogenesis, Prognosis and Therapy. *Cancers (Basel)* 2022;14:226.
5. Foerster F, Gairing SJ, Ilyas SI, et al. Emerging immunotherapy for HCC: A guide for hepatologists. *Hepatology* 2022;75:1604-26.
6. Fridman WH, Zitvogel L, Sautès-Fridman C, et al. The immune contexture in cancer prognosis and treatment. *Nat Rev Clin Oncol* 2017;14:717-34.
7. Mai J, Hua X, Bian ZH, et al. Identification of prognostic immune cells and potential immune-related markers in hepatocellular carcinoma. *Transl Cancer Res* 2022;11:2262-74.
8. Abdel Ghafar MT, Morad MA, El-Zamarany EA, et al. Autologous dendritic cells pulsed with lysate from an allogeneic hepatic cancer cell line as a treatment for patients with advanced hepatocellular carcinoma: A pilot study. *Int Immunopharmacol* 2020. [Epub ahead of print]. doi: 10.1016/j.intimp.2020.106375.
9. Grootaert H, Van Landuyt L, Hulpiau P, et al. Functional exploration of the GH29 fucosidase family. *Glycobiology* 2020;30:735-45.
10. Liu TW, Ho CW, Huang HH, et al. Role for alpha-L-fucosidase in the control of *Helicobacter pylori*-infected gastric cancer cells. *Proc Natl Acad Sci U S A* 2009;106:14581-6.
11. Waidely E, Al-Youbi AO, Bashammakh AS, et al. Alpha-L-Fucosidase Immunoassay for Early Detection of Hepatocellular Carcinoma. *Anal Chem* 2017;89:9459-66.
12. Liu S, Wang W, Zhao Y, et al. Identification of Potential Key Genes for Pathogenesis and Prognosis in Prostate Cancer by Integrated Analysis of Gene Expression Profiles and the Cancer Genome Atlas. *Front Oncol* 2020;10:809.
13. Uhlen M, Zhang C, Lee S, et al. A pathology atlas of the human cancer transcriptome. *Science* 2017;357:eaan2507.
14. Chandrashekar DS, Bashel B, Balasubramanya SAH, et al. UALCAN: A Portal for Facilitating Tumor Subgroup

- Gene Expression and Survival Analyses. *Neoplasia* 2017;19:649-58.
15. Bader GD, Hogue CW. An automated method for finding molecular complexes in large protein interaction networks. *BMC Bioinformatics* 2003;4:2.
 16. Subramanian A, Tamayo P, Mootha VK, et al. Gene set enrichment analysis: a knowledge-based approach for interpreting genome-wide expression profiles. *Proc Natl Acad Sci U S A* 2005;102:15545-50.
 17. Newman AM, Liu CL, Green MR, et al. Robust enumeration of cell subsets from tissue expression profiles. *Nat Methods* 2015;12:453-7.
 18. Li T, Fu J, Zeng Z, et al. TIMER2.0 for analysis of tumor-infiltrating immune cells. *Nucleic Acids Res* 2020;48:W509-14.
 19. Ru B, Wong CN, Tong Y, et al. TISIDB: an integrated repository portal for tumor-immune system interactions. *Bioinformatics* 2019;35:4200-2.
 20. Zhang Y, Zhang X, Kuang M, et al. Emerging Insights on Immunotherapy in Liver Cancer. *Antioxid Redox Signal* 2022;37:1325-38.
 21. Fang C, Liu S, Feng K, et al. Ferroptosis-related lncRNA signature predicts the prognosis and immune microenvironment of hepatocellular carcinoma. *Sci Rep* 2022;12:6642.
 22. Li YR, Chen JD, Zhu YY, et al. Evaluation of nuclear PGAM2 value in hepatocellular carcinoma prognosis. *Anticancer Drugs* 2022;33:e500-6.
 23. Yu X, Zhang R, Yang T, et al. Alpha-L-fucosidase: a novel serum biomarker to predict prognosis in early stage esophageal squamous cell carcinoma. *J Thorac Dis* 2019;11:3980-90.
 24. Yang F, Cui P, Lu Y, et al. Requirement of the transcription factor YB-1 for maintaining the stemness of cancer stem cells and reverting differentiated cancer cells into cancer stem cells. *Stem Cell Res Ther* 2019;10:233.
 25. Lee TK, Guan XY, Ma S. Cancer stem cells in hepatocellular carcinoma - from origin to clinical implications. *Nat Rev Gastroenterol Hepatol* 2022;19:26-44.
 26. Andre F, Mardis E, Salm M, et al. Prioritizing targets for precision cancer medicine. *Ann Oncol* 2014;25:2295-303.
 27. Hao X, Sun G, Zhang Y, et al. Targeting Immune Cells in the Tumor Microenvironment of HCC: New Opportunities and Challenges. *Front Cell Dev Biol* 2021;9:775462.
 28. Gibson EM, Nagaraja S, Ocampo A, et al. Methotrexate Chemotherapy Induces Persistent Tri-gliai Dysregulation that Underlies Chemotherapy-Related Cognitive Impairment. *Cell* 2019;176:43-55.e13.
- (English Language Editors: N. Korszniak and J. Gray)

Cite this article as: Hu Y, Tang D, Zhang P. Prognostic and immunological role of alpha-L-fucosidase 2 (*FUCA2*) in hepatocellular carcinoma. *Transl Cancer Res* 2023;12(2):257-272. doi: 10.21037/tcr-22-1850